Siderophore Production by a Rhizosphere-Associated *Streptomyces* from *Cyperus virens*

Phoebe Dennison[a], Robert Samples[b], Riccardo Racicot[b], & Lesley-Ann Giddings[a,b]*

[a]Department of Chemistry, Smith College, Northampton, MA
[b]Biochemistry Program at Smith College, Northampton, MA

https://doi.org/10.33697/ajur.2025.158

*Student: pdennison@smith.edu**
Mentor: lgiddings@smith.edu

ABSTRACT
Rhizosphere microbiomes produce iron chelators or siderophores to capture ferric iron, an essential nutrient for growth that is not always bioavailable. Plants with siderophore activity aid in phytoremediation by removing heavy metals and other pollutants. The *Cyperus* genus of plants has a high affinity for iron uptake in the phytoremediation of wastewater. Herein, we isolated a siderophore-producing microbe from the rhizosphere of *Cyperus virens*, an understudied member of this genus, using the Chrome Azurol S (CAS) assay. While this isolate has siderophore activity, it did not exhibit antimicrobial activity when plated on *Aspergillus niger, A. flavus*, or *Bacillus subtilis*. The isolate was identified as *Streptomyces* sp. PD-S100-1 through genomic sequencing and de novo assembly with a draft genome size of 8.2 Mbp and 73% GC content. antiSMASH analysis of the genome identified several siderophore biosynthetic gene clusters, including those involved in the production of mirubactin A and bacillibactin. Liquid chromatography-mass spectrometry (LC-MS) detected several siderophores, including mirubactin A–D, enterobactin, and other catecholates from these siderophore families. The positive CAS assay, siderophore gene cluster identification, and LC-MS/MS analyses show that the rhizosphere of *C. virens* contains siderophore-producing bacteria. Most detected metabolites, including enterobactin, increased in the presence of cerium, a lanthanide involved in the expression of secondary metabolites, whereas mirubactin production was reduced. The presence of rhizosphere siderophore-producing bacteria suggests that *C. virens* may have potential applications in environmental phytoremediation, targeting pollutants from wastewater, mining, agriculture, and energy production.

KEYWORDS
Siderophore; Mirubactin A; Enterobactin; Bacillibactin; Rhizosphere; *Cyperus virens*; *Streptomyces*; CAS Assay

INTRODUCTION

Iron is an essential nutrient for plants and microorganisms, but its bioavailability is highly oxidation state-dependent. Ferrous iron (Fe^{2+}) is more bioavailable, while ferric iron (Fe^{3+}) has greater biochemical importance, but is only water-soluble at concentrations up to 10^{-9} M.[1] Most bacteria require 10^{-6} M of intracellular Fe^{3+} for viability and produce siderophores, low molecular weight iron-chelating molecules that mediate ferric iron uptake.[1] There are four main types of siderophores: hydroxamates, catecholates, carboxylates, as well as numerous mixed-type siderophores with various metal binding moieties.[1] The most common class of siderophores in nature is the hydroxamates (e.g., ferrioxamine in **Figure 1)**, which are produced by both bacteria and fungi.[2]

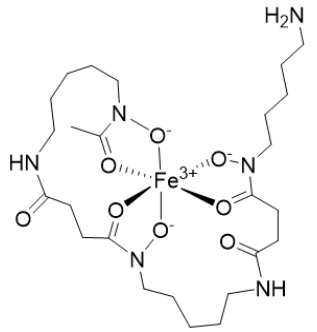

Figure 1. Structure of the hydroxamate siderophore ferrioxamine in complex with Fe^{3+}.

The metal-chelating capabilities of siderophores have applications in medicine, agriculture, and environmental protection. Siderophore-producing plants and microbes can be used to remediate natural or anthropogenic heavy metal contamination by

binding metals, reducing their bioavailability in soil.[1] These bacteria can be found in the plant rhizosphere to help regulate plant growth. Actinobacteria are ubiquitous taxa in the rhizosphere and are one of the most important sources of secondary metabolites, including siderophores.[3] For example, Wang *et al.* found that 44% of actinobacterial rhizosphere isolates produce siderophores.[3]

The application of siderophores in environmental protection through phytoremediation is of utmost importance today, with the continuing development and usage of natural land by humans. The misuse of land and waterways can lead to environmental damage and health issues. To ameliorate the negative effects of heavy metal and oil pollution, the use of plants in phytoremediation is a cost-effective and less complicated strategy than traditional methods, such as excavation, filtration, and adsorption.[4,5] Members of the *Cyperus* genus have been studied for their uptake of heavy metals in the environment. For example, *Cyperus esculentus* can grow in wetlands of wastewater and accumulate heavy metals in its roots with the highest affinity for iron uptake.[6] Understanding more about the siderophore activity of plants to undo or prevent environmental damage is pertinent.

C. virens is a grass-like sedge plant (**Figure 2**) that has not been explored for phytoremediation but holds unconsidered potential as other genus members have successfully been applied in phytoremediation.[7] It is typically found in the southeastern states of the US in moist places like marshes and globally in tropical and subtropical areas of the Americas.[8–10] Within its larger family of *Cyperaceae*, specifically of *Costularia*, 52% of isolated bacterial strains were reported to produce siderophores.[9] Additionally, *Cyperaceae* are commonly found in nutrient-deficient environments,[1] suggesting that the presence of siderophore-producing bacteria is essential for the growth of plants in this family, including *C. virens*. No siderophore activity has been reported from *C. virens* rhizosphere bacteria, making this study an important addition to understanding more about this specific plant and the *Cyperus* genus.

Figure 2. The *C. virens* plant from the Lyman Plant House at Smith College in Northampton, MA.

We hypothesized that the *C. virens* rhizosphere contains actinobacteria that produce siderophores that may be related to the host plant's phytoremediation capabilities. These rhizosphere bacteria may also produce higher yields, a greater diversity, or chemically unique siderophores. To determine siderophore activity in the rhizosphere of *C. virens,* microbial isolation was performed using glucose-yeast-malt (GYM) agar and marine agar to enrich for actinobacteria, which were then analyzed for the presence of siderophores using a Chrome Azurol S (CAS) assay. A draft genome was obtained for an isolate to identify specific gene clusters related to siderophores and other bioactive properties. Liquid chromatography-mass spectrometry (LC-MS) analyses of the isolate grown in the presence and absence of cerium, a strong inducer of secondary metabolites, were performed to detect changes in siderophore production and gain insight into the regulation of their biosynthesis.[11]

METHODS AND PROCEDURES

Plant Sampling and Processing

The roots and rhizosphere of *C. virens* were collected from the Lyman Plant House and Conservatory at Smith College in Northampton, Massachusetts. Root pieces (~2 g) were separated from the soil and baked at 50 °C for 30 minutes to select for heat-resistant, Gram-positive actinobacteria. Baked roots were pestled with autoclaved water to make a root solution (0.25 g root/mL). Soil (<1 g) was baked at 50 °C for 30 minutes and then combined with autoclaved water (0.1 g soil/mL) for one hour of rehydration on a slow stirring plate.

Isolation and Cultivation

Root and soil solutions were serially diluted (10^0 up to 10^{-2}) with autoclaved water. Solutions were mixed, centrifuged at 6000 x *g* for three minutes, and spread (100 µL) on solid glucose, yeast extract, and malt extract (GYM) media containing glucose (4 g/L), agar (10 g/L; BD Biosciences, Franklin Park, NY), yeast extract (4 g/L), and malt extract (2 g/L) with nalidixic acid (20 mg/L, NDA) and cycloheximide (80 mg/L, CHX). Plates were incubated for one week at 37 °C. Marine agar plates (BD Biosciences, Franklin Park, NY) were also prepared using the aforementioned dilution series.

Chrome Azurol S, Antibacterial, and Antifungal Assays

CAS dye was prepared according to the procedure by Louden, et. al.[12] The CAS mixture was poured over the isolate on GYM-NDA-CHX and marine agar plates and incubated at room temperature. For antibacterial and antifungal assays, GYM plates were also spread with either of the following: *Bacillus subtilis, Aspergillus flavus,* and *A. niger*. Cell scrapings of isolates were dropped onto these plates, incubated at 37 °C, and analyzed for zones of inhibition.

DNA Extraction, Library Preparation, and Illumina Sequencing

The extraction of genomic DNA (~20 mg) from cells on GYM agar was performed using the ZymoBIOMICS DNA microprep kit per the manufacturer's instructions. Using the 2 x 151 paired base end NEBNext UltraExpress FS Library Prep Kit (Ipswich, MA), a library of the extracted DNA was prepared from the isolate per the manufacturer's instructions. The quality of the library was assessed using the Fragment Analyzer 5200. The concentration of the library was confirmed using the Qubit 4. The DNA library was sequenced at the Center for Molecular Biology at Smith College using an Illumina MiSeq (San Diego) and MiSeq reagent Kit V3 (600-cycle).

De Novo Genome Assembly and Bioinformatic Analysis

The sequenced genome was uploaded to Galaxy (version 24.1, accessed November 2024), and the reads were combined using the concatenate multiple datasets (Galaxy Version 1.4.3, accessed November 2024) tool.[13] Low-quality trims were eliminated using the Trimmomatic (Galaxy Version 0.39+galaxy2, accessed November 2024) tool.[14] The quality of reads was analyzed using the FastQC (Galaxy Version 0.74+galaxy1, accessed November 1, 2024) tool.[15] The data was assembled using Unicycler (Galaxy version 0.5.1+galaxy0, accessed November 2024) and the resulting assembly was submitted to GenBank.[16] Genome assembly quality was assessed by Quast Galaxy Version 5.2.0+galaxy1 (accessed November 3, 2024) tool, which also determined the number of contigs.[17–20] The taxonomic identification of the sample was completed using NCBI BLAST + blastn (Galaxy version 2.14.1+galaxy2, accessed November 2024) tool, where the entire genome assembly was compared against the NCBI Whole-Genome-Shotgun contigs database.[21–23] Furthermore, Sanger sequencing of the partial bacterial 16S rRNA gene using 27F and 1492 primers further confirmed the taxonomic identification.[23] Due to the challenging taxonomic identification of *Streptomyces* via 16S ribosomal RNA gene sequencing, a set of established target genes (23S rRNA, groEL, 16S rRNA, rpoB, recA, gyrB, ssr1A, secA, cox1B, and trpB) along with the largest contig were blasted against the NCBI core NT database for taxonomic identification.[24] The RAST annotation tool was used to visualize related functional genes coded as subsystems within the genome using the RASTtk feature.[25] The final assembled genome was annotated using Prokka (Galaxy Version 1.14.6+galaxy1, accessed November 2024).[26,27] Identification of secondary metabolites was completed using the antiSMASH (Galaxy Version 6.1.1+galaxy1, accessed November 2024) tool with default parameters.[28]

Liquid Cultivation for LC-MS/MS

Liquid GYM media (10 mL) was inoculated with cell scrapings. A cerium edetate stock solution (50 mM) was prepared with equal volumes of aqueous stocks of $CeCl_3 \cdot 7\ H_2O$ (100 mM; Sigma-Aldrich, St. Louis, MO, USA) and disodium ethylenediaminetetraacetic (100 mM; Sigma-Aldrich, St. Louis, MO, USA). Using a 96-well plate, three culture replicates were used for the following condition and incubated for seven days at 30 °C stationary: GYM media (control; 200 µL); GYM (180 µL) with inoculant (20 µL); and GYM (160 µL) with inoculant (20 µL) and NaCe-EDTA (2.5 mM, 20 µL).

Liquid Chromatography/Mass Spectrometry (LC/MS)

LC/MS grade methanol (200 µL) was added to cultures grown in the 96-well plate, sonicated for one minute, centrifuged for five minutes at 6000 x *g*, and analyzed by LC/MS. A Thermo Scientific (Waltham, MA) Q-exactive HF-X Hybrid Quadrupole-Orbitrap mass spectrometer interfaced with a Vanquish Horizon Ultra High Performance Liquid Chromatography (UHPLC) system and VH-D10-A UV detector using a Waters (Milford, MA) HSS T3 C18 column (1.8 µm, 2.1 × 150 mm) was used for analysis. Using a flow rate of 0.5 mL min-1, samples (2 µL) were injected onto the column with a maintained chamber temperature of 40 °C. UHPLC separation was achieved using the following gradient method: 2% acetonitrile: 98% water with 0.1% formic acid for 1 min, 2–40% over 4 min, 40–98% over 3 min, 98–2% over 0.2 min, and 2% for 2 min. The UV-vis data were collected with 200–300, 300–400, 400–500, and 500–600 nm channels. The following electrospray ionization (ESI) settings were used in probe position D: 40 sheath gas flow, 8 auxiliary gas flow, 1 sweep gas flow, 3.5 kV spray voltage, 380 °C capillary

temperature, 50 radiofrequency (RF) funnel level, and 350 °C auxiliary gas temperature. A Top 5 DDA method was used with MS1 (60,000 resolution) and MS2 (15,000 resolution) scans between 150-2,000 m/z.

LC-MS/MS Data Analysis

For untargeted metabolomic analyses, raw data was processed in MS-DIAL v5.5.241113 with default settings,[29] profile data for MS1 and MS2, [M+H] and [M+Na] adducts selected, a minimum peak picking threshold of 3e5 and peak lists analyzed with MPACT v1.00 r24.11.17.[30] Data was filtered and visualized with default settings in MPACT. Targeted analysis was conducted in Thermo Freestyle 1.8 SP2 and MS/MS spectra matches were confirmed using NIST 23 and/or GNPS reference spectral libraries.[31]

Data Sharing and Nucleotide Accession Numbers

Genome assembly and metadata were submitted to the National Center for Biotechnology Information under BioProject identifier PRJNA1212226.

RESULTS

Colony Growth and Morphology on GYM-NDA-CHX and Marine Media

Bacterial colonies were selected based on their resemblance to actinobacteria on GYM-NDA-CHX media (**Figure 3**). PD-S100-1 on GYM-NDA-CHX media formed small grayish/white colonies with no diffusible pigment. Colonies were convex in elevation with a dry, fuzzy texture—an indication of sporulating ability. PD-S100-1 also grew on high-salinity marine media but changed from beige small colonies to punctiform colonies.

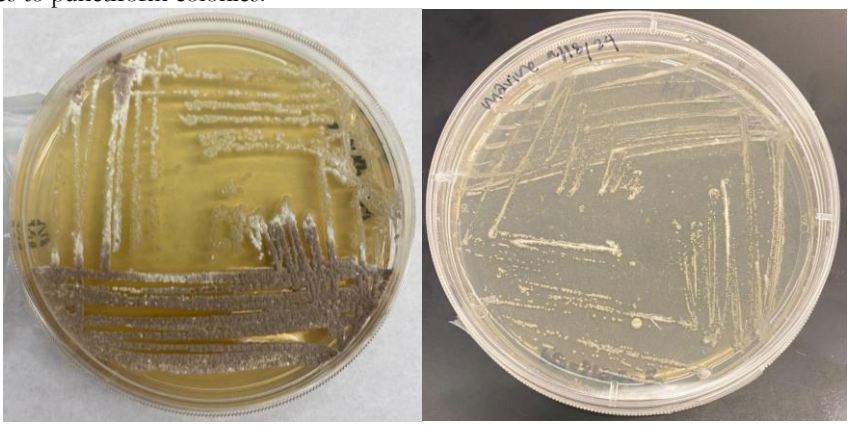

Figure 3. Isolation of PD-S100-1 on GYM-NDA-CHX media (left), showing a higher density of pigmented colonies with increasingly dry texture. PD-S100-1 on high-salinity marine media (right) grows as smaller colonies.

CAS Assay

CAS assays detected the production of siderophores by bacterial colonies. Isolate PD-S100-1 exhibited a density-dependent orange color change on the CAS assay plate, which had the highest colony density (**Figure 4**). The bright orange indicated the isolate was a strong siderophore producer.

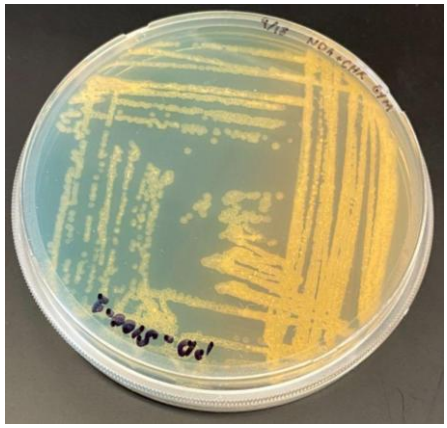

Figure 4. Image of CAS plate assay with isolate PD-S100-1 showing density-dependent siderophore production.

Antifungal and Antibacterial Assays

The antibacterial and antifungal activities were evaluated using *A. flavus*, *A. niger*, and *B. subtilis* on GYM plates. PD-S100-1 showed no antibacterial activity against *B. subtilis*. PD-S100-1 grew on plates inoculated with both of the following fungi: *A. niger* and *A. flavus*.

Genomic Sequencing, Taxonomic Identification, and Secondary Metabolites

A draft genome of PD-S100-1 was obtained and found to be 8.2 Mbp with a 73% GC content. The total number of reads was 1,674,272, and 1,644,916 reads passed quality control. The genome assembly is made up of 261 contigs per the Quast tool and the N50 was 51,839 bp. The isolate was identified as *Streptomyces* sp. When the whole genome and phylogenetic gene markers were compared to NCBI genomic databases. All phylogenetic gene markers were >91% identical to other strains of *Streptomyces*, and the largest contig (30,632 base pairs) was 99.4% identical to *Streptomyces* sp. E14 cont1.653 (See **Supporting Information Tables 1–2**). RAST annotation of the biological functions of this genome (**Figure 5**) revealed that most genes were involved in cellular respiration, phosphorus metabolism, and stress responses. There were also several genes involved in iron acquisition and secondary metabolism.

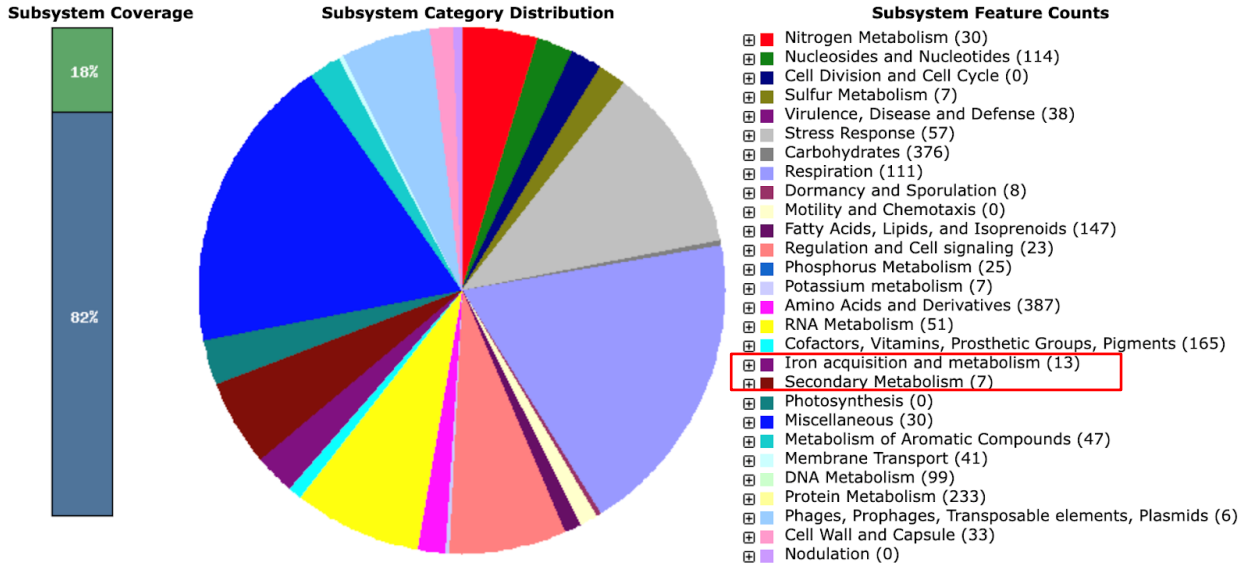

Figure 5. RAST annotation of *Streptomyces* sp. PD-S100-1 genome, indicating related functional roles of genes.[23] The percentage of genes that could be grouped within a subsystem (18%) is shown in green and the percentage of genes that could not be classified (82%) is shown in blue. Feature counts involved in iron acquisition and secondary metabolism are within the red box.

Region	Type	Most Similar Gene Cluster	Similarity
11.1	NRPS	Mirubactin	50%
12.1	Siderophore		
16.1	Terpene	Albaflavenone	100%
21.1	Lanthipeptide-class-iii, RiPP-like	Informatipeptin	100%
51.1	Siderophore		
54.1	NRPS, RiPP-like	Bacillibactin	100%
57.1	Terpene	Hopene	92%
140.1	Terpene	Geosmin	100%
148.1	Ectoine	Ectoine	100%

Table 1. Select identified biosynthetic gene clusters from genomic sequencing of isolate PD-S100-1. 'Region' indicates the string of predicted Pfam domains fed into a hidden Markov model within the antiSMASH pipeline based on the location of the gene cluster within the genome. 'Type' and 'Most Similar Gene Cluster' indicate the class of secondary metabolite and the highest ranked gene cluster, respectively. The ranking system is a composite score based on the number of query and core query genes with a significant hit, gene pairs with conserved synteny as well as those involving a core gene as well as the presence or absence of a core gene. The similarity percentage is the percentage of genes within the known gene cluster with some match to at least one gene within the query region. Only the most similar gene clusters with at least 50% similarity to known gene clusters were included.

antiSMASH identified and annotated twenty-eight secondary metabolite gene clusters in the PD-S100-1 genome. These gene clusters are involved in the production of diverse classes of natural products, including terpenes, siderophores, nonribosomal peptides (NRPs), polyketides, lanthipeptides, and ribosomally synthesized and posttranslationally modified peptide products (RiPPs) with varying degrees of similarity to the sequenced genome of PD-S100-1 (**Supporting Information Table 3**). Four siderophore biosynthetic gene clusters were identified. Genes involved in the biosynthesis of ficellomycin and grincamycin had low similarity, while those involved in the biosynthesis of mirubactin A and bacillibactin were higher in similarity (**Table 1**). Notably, several gene clusters were 100% identical to known genes involved in the production of albaflavenone, informatipeptin, bacillibactin, hopene, geosmin, and ectoine (**Table 1**).

Siderophores detected by LC-MS

Metabolomics was performed on extracts of PD-S100-1 grown in the presence and absence of cerium. Among the features putatively identified are the catecholate siderophore enterobactin, mirubactin A, and three degradation/cyclization products (**Figure 6**). Enterobactin as well as mirubactins B and D were significantly upregulated by cerium elicitation, while mirubactins B and C were downregulated or unchanged.[32]

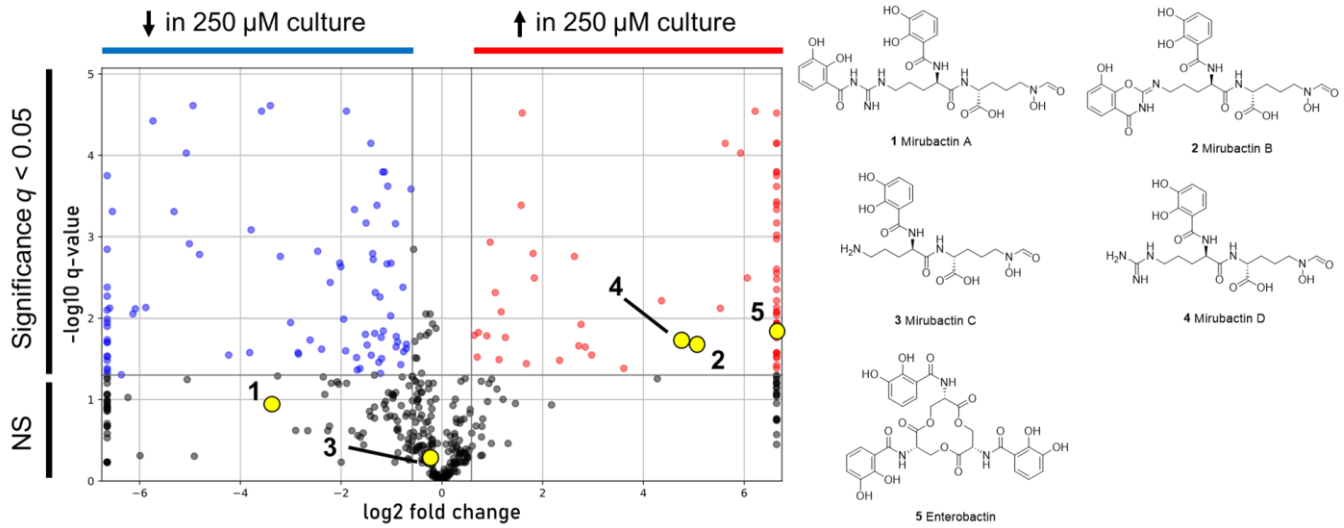

Figure 6. Volcano plot of the LC-MS features in the *Streptomyces* sp. PD-S100-1, with features significantly upregulated in the cerium treatment shown in red, and features significantly downregulated shown in blue. Filled yellow circles indicate features associated with numbered compounds and their structures are shown on the right.

Fragmentation analysis identified the presence of siderophores enterobactin (670.1517 *m/z*, 670.152047 *m/z* calculated for [M+H]) and mirubactin A (605.2199 *m/z*, calculated 605.220734 for [M+H]) (**Figure 7**). The experimental MS/MS fragmentation pattern of mirubactin A contained several peaks characteristic of the compound, including key fragments at 469.2039 *m/z*, 333.1879 *m/z*, and 293.1233 *m/z*. Enterobactin was likewise confirmed based on its MS/MS fragmentation pattern with key peaks at 224.0553 *m/z* and 137.0232 *m/z*. Mirubactin A production was downregulated with cerium treatment, whereas enterobactin production was exclusively produced in the presence of cerium.

Several other catecholates were detected by LC-MS/MS, confirming the presence of siderophores from the enterobactin and mirubactin families (**Table 2**). Further investigation of compounds possessing the characteristic 137.0233 *m/z* dihydroxybenzoyl fragment revealed the presence of the recently reported mirubactin A decomposition products, mirubactins B-D at higher levels in the cerium-elicited culture (**Figure 8**).[32]

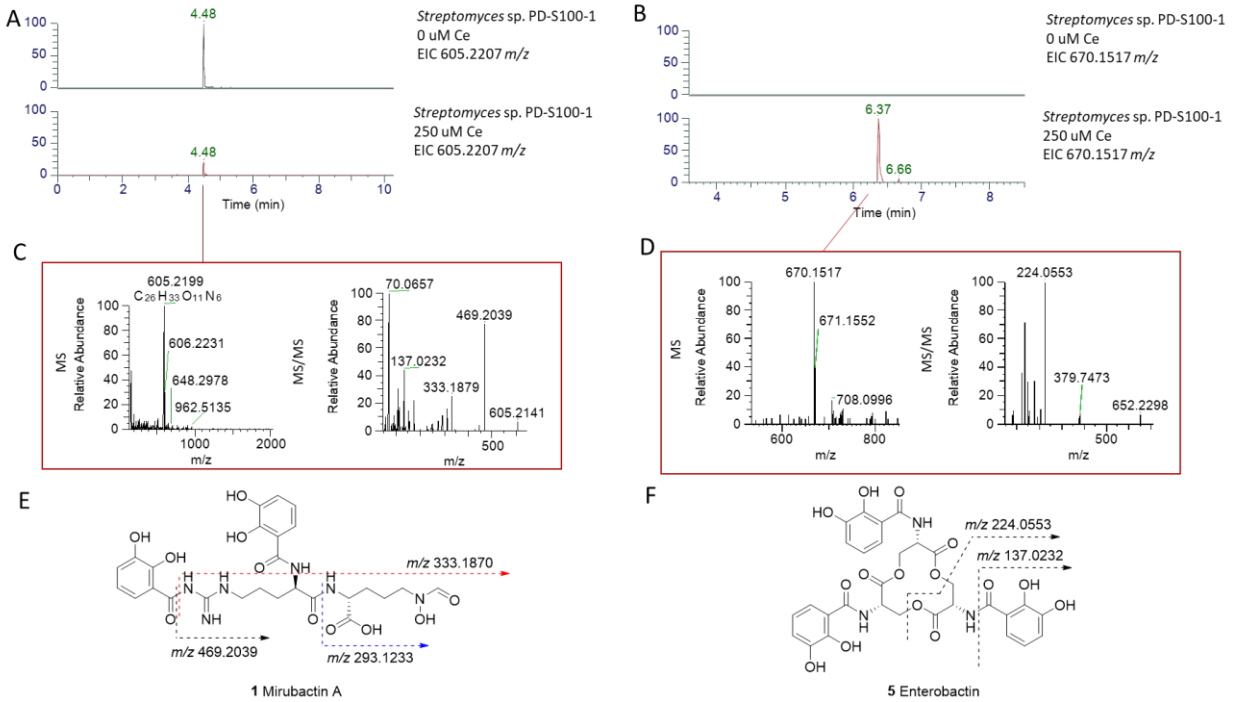

Figure 7. Confirmation of siderophore production by mass spectrometry. Extracted ion chromatograms confirming the production of mirubactin A (left) and enterobactin (right) (A), MS and MS/MS fragmentation (B), and molecular structure with proposed fragmentation pathways (C).

Compound	Retention Time (minutes)	Theoretical [M+H]	Experimental *m/z*
2,3-dihydroxy-*N*-benzoylserine trimer	5.67	688.16261	688.1616
2,3-dihydroxy-*N*-benzoylserine dimer	4.94	465.1145	465.1138
Fimsbactin A	4.70	575.1989	575.1985
Enterobactin	6.37	670.1521	670.1517
Mirubactin A	4.48	605.2207	605.2199
Mirubactin B	4.69	588.1941	588.1935
Mirubactin C	3.25	427.1829	427.1820
Mirubactin D	3.43	469.2036	469.2043

Table 2. Catecholate siderophores confirmed by LC-MS/MS.

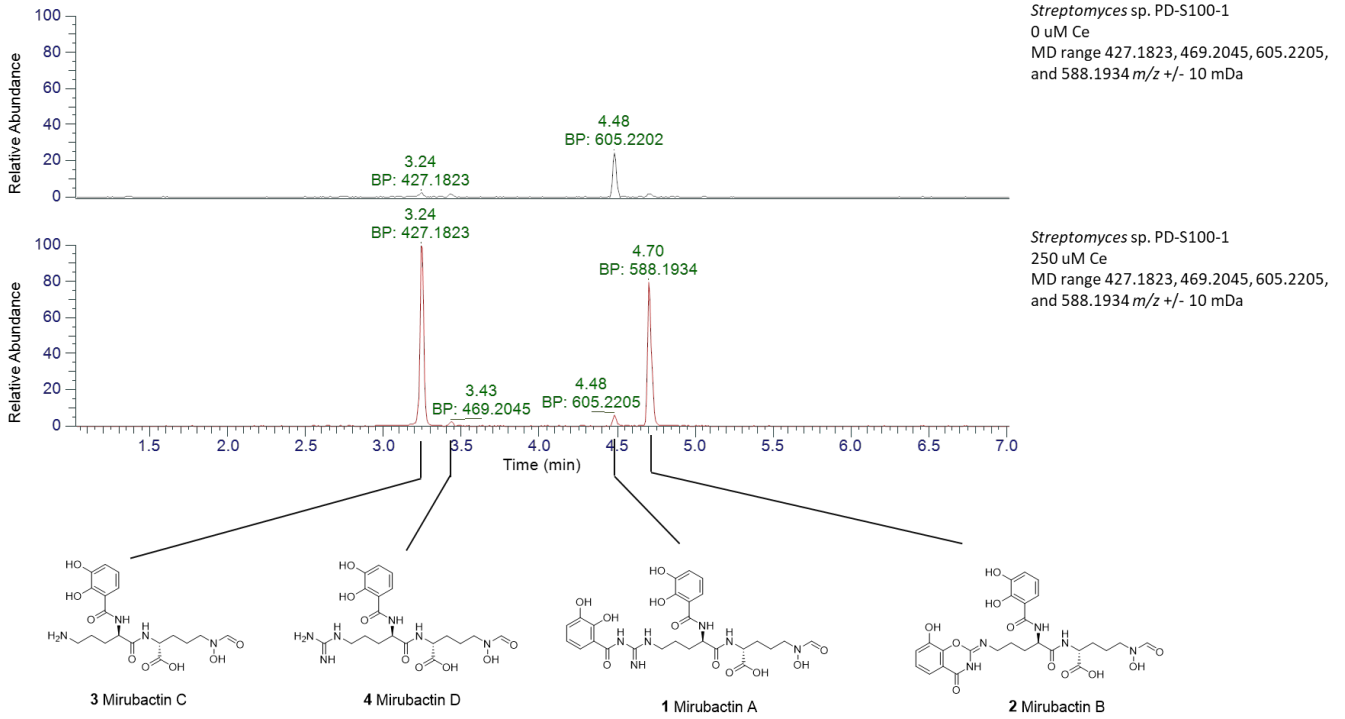

Figure 8. Preliminary extracted ion chromatograms of mirubactin A and its decomposition products in control and cerium-elicited cultures of *Streptomyces sp.* PD-S100-1 showing the marked decrease in mirubactin A in elicited cultures is accompanied by increases in the decomposition products, mirubactins B-D.

DISCUSSION

Phytoremediation involves plants absorbing metals from their roots, oftentimes with the help of bacteria, and accumulating or incorporating them into the plant metabolome.[33] Members of the *Cyperaceae* family have been reported to host siderophore-producing bacteria. Thus, *C. virens* was hypothesized to contain siderophore-producing bacteria in its rhizosphere that may play a role in phytoremediation.[34] Actinobacteria are prolific producers of siderophores; thus, we aimed to identify these bacteria in the *C. virens* rhizosphere.

Sporulating bacteria were preselected from the rhizosphere using a heat treatment as well as selecting for Gram-positive bacteria through the use of NDA and CHX. The PD-S100-1 isolate grew on both GYM-NDA-CHX and marine media plates (**Figure 3**), revealing its salt tolerance.[35] *C. virens* grows in the (sub)tropics of the Americas, where it may inhabit brackish environments, hence its ability for bacteria from its rhizosphere to grow in high salinity media.[8] However, the colonies were fewer in number when the same volume of cells were plated, suggesting that these isolates are salt-tolerant and high-salinity environments decrease growth.

Bacterial siderophore production was confirmed by CAS assays containing a blue iron-chelating dye that turns orange when a molecule outcompetes it for binding iron.[12] While PD-S100-1 displayed no CAS activity on marine agar, the isolate displayed strong density-dependent siderophore production on GYM-NDA-CHX media (**Figure 4**), suggesting the involvement of an autoregulator quorum sensing molecule in the regulation of siderophore production.[36,37] High salinity environments put stress on bacteria, and the larger plant, which may lead to decreased siderophore production; hence, the lack of CAS activity on marine agar.[38] A large orange halo developed around PD-S100-1 in the CAS assay (**Figure 4**), indicating siderophore production. While this is the first report of a siderophore producer within the *C. virens* rhizosphere, siderophore production has been previously reported by the rhizosphere of other strains from the *Cyperus* genus using the CAS assay.[39] However, no significant antimicrobial activity against *Aspergillus niger*, *A. flavus*, or *B. subtilis* was observed, even though Gram-positive bacteria have been reported to be sensitive to extracts from *Cyperus* plants.[40]

Whole genome sequencing revealed PD-S100-1 contained siderophore biosynthetic genes and determined the taxonomic identification of this isolate to be *Streptomyces* sp. PD-S100-1. The high GC content is consistent with actinobacteria, as percentages over 70% often indicate *Streptomyces*.[41] Of the 28 identified biosynthetic gene clusters, only a few gene clusters were similar to those involved in the production of important bioactive molecules. Four siderophore-producing gene clusters were

identified and two were predicted to produce mirubactin A and bacillibactin (**Figure 9**). The other two gene clusters were annotated as siderophore biosynthetic gene clusters based on sequence alignments of experimentally characterized proteins and protein domains but make products unlike any known siderophores, indicating the potential of PD-S100-1 to produce new chemistry. Mirubactin A and bacillibactin biosynthetic gene clusters were higher in similarity to genes known to be involved in their biosynthesis (**Table 1, Figure 9**)[42,43], and both compounds are catecholates consisting of dihydroxybenzoic acid (DHBA) functionalized scaffolds that display strong siderophore activity.[44] Mirubactin A is not only a siderophore, but it also promotes cell wall growth, whereas bacillibactin has antibacterial and antifungal properties.[45,46] The bacillibactin gene cluster may not be expressed under these conditions due to the lack of antimicrobial activity detected under these growth conditions. The identification of these siderophore biosynthetic gene clusters supports the results of the CAS assay and suggests that PD-S100-1 has the potential to produce novel siderophores.

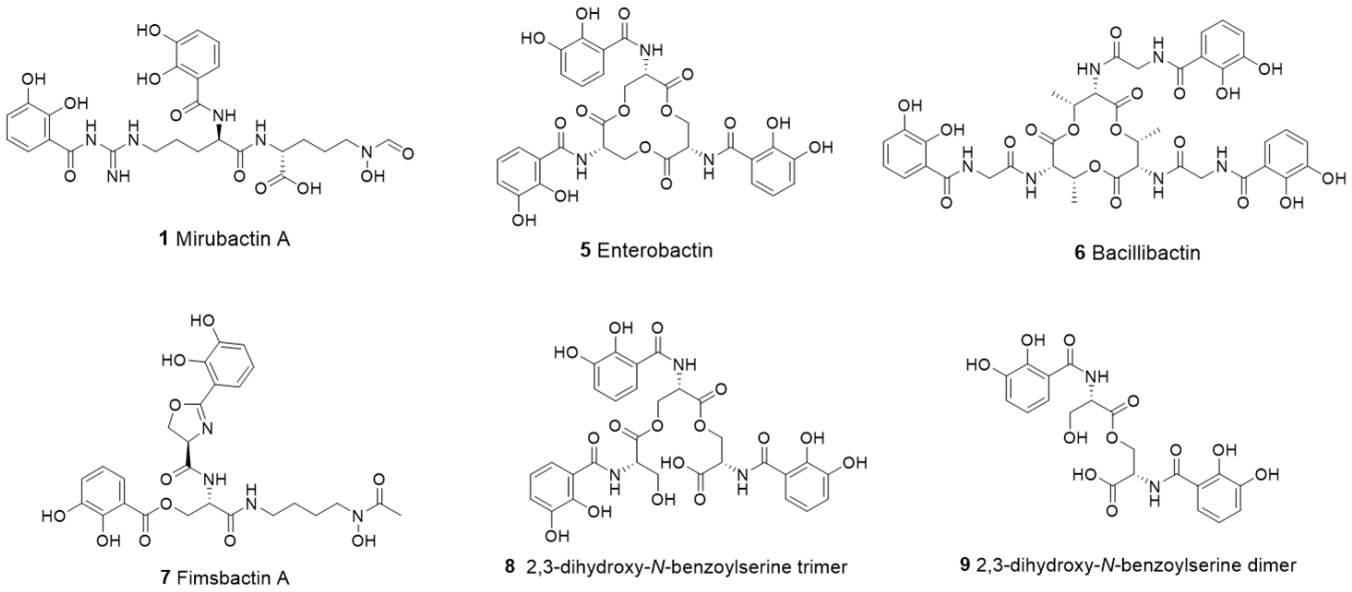

Figure 9. Structures of key catecholate siderophores or families thereof identified in *Streptomyces* sp. PD-S100-1 or its genome using LC-MS/MS.

Several catecholate siderophores were identified by LC-MS (**Table 2**), including the decomposition products of mirubactin A, mirubactins B-D (**Figures 6–9**). The detection of the mirubactins along with their corresponding biosynthetic gene cluster confirmed that this siderophore is produced by *Streptomyces* sp. PD-S100-1, which is consistent with other reports of *Streptomyces* producing mirubactin A.[47] Additionally, the related hybrid siderophore fimsbactin A was detected (**Figure 9**). Most secondary metabolite production was upregulated (**Figure 7**) when *Streptomyces* sp. PD-S100-1 was grown in the presence of cerium, a rare earth element (REE) that can trigger the production of secondary metabolites from biosynthetic genes not always expressed (i.e., cryptic metabolites).[11] Interestingly, Khan *et al.* found that multiple members of the *Cyperus* genus accumulate or tolerate REEs, which may also occur when PD-S100-1 is grown in the presence of *C. virens* and cerium.[48] The addition of low concentrations of REEs has been shown to have beneficial effects on the growth of many plants, including increasing their iron uptake.[48]

The observed decrease in mirubactin A in cultures treated with cerium was unexpected, as significant increases in enterobactin were detected and both of these molecules are catecholates (**Figure 6**). Furthermore, increases in mirubactins B-D, known decomposition products of mirubactin A,[32] were also observed, suggesting that cerium may not decrease the production of mirubactins but rather accelerate their decomposition to a diverse set of related hydroxamate siderophores. It is unclear if this finding has practical implications for the metal-chelating phenotype of *Streptomyces sp.* PD-S100-1. However, mirubactins C-D were reported to exhibit reduced iron complexing capability and the unusual cyclic amide moiety in mirubactin B may modulate its metal chelation profile.[32]

Enterobactin was detected in extracts of PD-S100-1 (**Figure 6–7**), which has also been reported in two other *Streptomyces* species.[49] Although enterobactin was produced, it was challenging to identify its biosynthetic gene cluster. While the NRPS modules in the annotated bacillibactin gene cluster putatively code only for serine and dihydrobenzoic acid (DHBA)—which is congruent with enterobactin rather than bacillibactin—the architecture of this gene cluster differed from other reported enterobactin gene clusters. While bacillibactin was not detected in extracts, the enterobactin gene cluster may be undetectable because it could be split between contigs or some functions of the biosynthetic gene cluster (i.e., shikimate synthesis) are provided by the mirubactin

biosynthetic machinery, rendering it as nonfunctional in the absence of another catecholate siderophore gene cluster. Enterobactin increased in the cerium treatment, following the overall trend of cerium positively impacting secondary metabolite regulation. Interestingly, mirubactin A was downregulated, whereas enterobactin was upregulated, as these belong to the same family of siderophores. It is unclear why there wasn't a similar increase in enterobactin's scaffold and DHBA hydrolysis like mirubactin A, though the cyclic scaffold of enterobactin may increase its stability relative to the linear mirubactin scaffold. Despite this, low levels of the DHBA-serine dimer and trimer, which may be hydrolysis products, were detected at low levels (**Table 2, Figure 9**).

PD-S100-1 not only produces catecholate siderophores but also has the genetic potential to make several other environmentally relevant secondary metabolites that were undetected under these growth conditions and LC/MS methods. For example, biosynthetic gene clusters dedicated to making the osmoregulator ectoine were identified. Ectoine can stabilize microorganisms under high osmotic stress conditions and prevent desiccation.[50] PD-S100-1 grew on the marine agar (**Figure 3**), and the ectoine gene cluster may enable it to overcome the environmental stress of the high salinity. Furthermore, other gene clusters were annotated as being involved in the production of the antimicrobials albaflavenone and informatipeptin.[51,52] While PD-S100-1 did not exhibit antibacterial or antifungal properties against *B. subtilis*, *A. niger*, and *A. flavus* under the growth conditions used, this gene cluster suggests possible antimicrobial activity of bacteria in the *C. virens* rhizosphere.

CONCLUSIONS

Streptomyces sp. PD-S100-1 was isolated from the *C. virens* rhizosphere and found to produce siderophores in CAS plate assays. The genome of this isolate was sequenced and found to contain biosynthetic gene clusters for antimicrobials, such as albaflavenone and informatipeptin, and siderophore production via mirubactin and bacillibactin, supporting the results from the CAS plate assays. Metabolomics connected genes to the actual molecules produced by *Streptomyces* sp. PD-S100-1, confirming the production of mirubactin A and enterobactin, among other catecholate members of their families. *Streptomyces* sp. PD-S100-1 may play useful roles in iron acquisition in *C. virens*. Importantly, linking biosynthetic genes to their producing metabolites provides opportunities to source metabolites, such as siderophores, and perform genetic manipulation to modify metabolite production, especially in the context of *Cyperus* phytoremediation.

ACKNOWLEDGMENTS

This work was supported by the Faculty Early Career Development (CAREER) Award from the National Science Foundation (NSF) (grant number 2236643 for P.D., R.S, R.R., and L-A.G.). We are also extremely grateful to Sophie Collet for assisting with the formatting of this manuscript.

Supporting information available here.

REFERENCES

1. Vijay, K., Shibasini, M., Sivasakthivelan, P., and Kavitha, T. (2023) Microbial siderophores as molecular shuttles for metal cations: sources, sinks and application perspectives, *Arch Microbiol* 205, 322. *https://doi.org/10.1007/s00203-023-03644-3*
2. Xie, B., Wei, X., Wan, C., Zhao, W., Song, R., Xin, S., and Song, K. (2024) Exploring the Biological Pathways of Siderophores and Their Multidisciplinary Applications: A Comprehensive Review, *Molecules* 29, 2318. *https://doi.org/10.3390/molecules29102318*
3. Wang, W., Qiu, Z., Tan, H., and Cao, L. (2014) Siderophore production by actinobacteria, *Biometals* 27, 623–631. *https://doi.org/10.1007/s10534-014-9739-2*
4. Basumatary, B., Bordoloi, S., and Sarma, H.P. (2012) Crude Oil-Contaminated Soil Phytoremediation by Using *Cyperus brevifolius* (Rottb.) Hassk, *Water Air Soil Pollut* 223, 3373–3383. *https://doi.org/10.1007/s11270-012-1116-6*
5. Senanu, L.D., Kranjac-Berisavljevic, G., and Cobbina, S.J. (2023) The use of local materials to remove heavy metals for household-scale drinking water treatment: A review, *Environmental Technology & Innovation* 29, 103005. *https://doi.org/10.1016/j.eti.2023.103005*
6. Chandra, R., and Yadav, S. (2011) Phytoremediation of Cd, Cr, Cu, Mn, Fe, Ni, Pb and Zn from Aqueous Solution Using Phragmites Cummunis, Typha Angustifolia and *Cyperus Esculentus*, *International Journal of Phytoremediation* 13, 580–591. *https://doi.org/10.1080/15226514.2010.495258*
7. de Souza, D.M., da Silva, J. de L., Ludwig, L. da C., Petersen, B.C., Brehm, F.A., Modolo, R.C.E., De Marchi, T.C., Figueiredo, R., and Moraes, C.A.M. (2023) Study of the phytoremediation potential of native plant species identified in an area contaminated by volatile organic compounds: a systematic review, *Int J Phytoremediation* 25, 1524–1541. *https://doi.org/10.1080/15226514.2023.2170974*
8. Tucker, G.C., Marcks, B.G., and Carter, J.R. *Cyperus virens* - FNA, *Flora North America*. http://floranorthamerica.org/Cyperus_virens
9. *Cyperus virens* Michx *USDA Plants Database*. https://plants.usda.gov/home/plantProfile?symbol=CYVI2

10. *Cyperus virens* Michx. *Royal Botanical Gardens Kew Plants of the Online World.* http://powo.science.kew.org/taxon/urn:lsid:ipni.org:names:306303-1

11. Tanaka, Y., Hosaka, T., and Ochi, K. (2010) Rare earth elements activate the secondary metabolite–biosynthetic gene clusters in *Streptomyces coelicolor* A3(2), *J Antibiot* 63, 477–481. *https://doi.org/10.1038/ja.2010.53*

12. Louden, B.C., Haarmann, D., and Lynne, A.M. (2011) Use of Blue Agar CAS Assay for Siderophore Detection, *Journal of Microbiology & Biology Education. https://doi.org/10.1128/jmbe.v12i1.249*

13. Goecks, J., Nekrutenko, A., Taylor, J., and The Galaxy Team (2010) Galaxy: a comprehensive approach for supporting accessible, reproducible, and transparent computational research in the life sciences, *Genome Biology* 11, R86. *https://doi.org/10.1186/gb-2010-11-8-r86*

14. Bolger, A.M., Lohse, M., and Usadel, B. (2014) Trimmomatic: a flexible trimmer for Illumina sequence data, *Bioinformatics* 30, 2114–2120. *https://doi.org/10.1093/bioinformatics/btu170*

15. Babraham Bioinformatics - FastQC A Quality Control tool for High Throughput Sequence Data https://www.bioinformatics.babraham.ac.uk/projects/fastqc/

16. Wick, R.R., Judd, L.M., Gorrie, C.L., and Holt, K.E. (2016) Unicycler: resolving bacterial genome assemblies from short and long sequencing reads. Preprint at bioRxiv, *https://doi.org/10.1101/096412 https://doi.org/10.1101/096412*

17. Mikheenko, A., Prjibelski, A., Saveliev, V., Antipov, D., and Gurevich, A. (2018) Versatile genome assembly evaluation with QUAST-LG, *Bioinformatics* 34, i142–i150. *https://doi.org/10.1093/bioinformatics/bty266*

18. Mikheenko, A., Valin, G., Prjibelski, A., Saveliev, V., and Gurevich, A. (2016) Icarus: visualizer for de novo assembly evaluation, *Bioinformatics* 32, 3321–3323. *https://doi.org/10.1093/bioinformatics/btw379*

19. Mikheenko, A., Saveliev, V., and Gurevich, A. (2016) MetaQUAST: evaluation of metagenome assemblies, *Bioinformatics* 32, 1088–1090. *https://doi.org/10.1093/bioinformatics/btv697*

20. Gurevich, A., Saveliev, V., Vyahhi, N., and Tesler, G. (2013) QUAST: quality assessment tool for genome assemblies, *Bioinformatics* 29, 1072–1075. *https://doi.org/10.1093/bioinformatics/btt086*

21. Altschul, S.F., Madden, T.L., Schäffer, A.A., Zhang, J., Zhang, Z., Miller, W., and Lipman, D.J. (1997) Gapped BLAST and PSI-BLAST: a new generation of protein database search programs, *Nucleic Acids Research* 25, 3389–3402. *https://doi.org/10.1093/nar/25.17.3389*

22. Camacho, C., Coulouris, G., Avagyan, V., Ma, N., Papadopoulos, J., Bealer, K., and Madden, T.L. (2009) BLAST+: architecture and applications, *BMC Bioinformatics* 10, 421. *https://doi.org/10.1186/1471-2105-10-421*

23. Cock, P.J.A., Chilton, J.M., Grüning, B., Johnson, J.E., and Soranzo, N. (2015) NCBI BLAST+ integrated into Galaxy, *GigaScience* 4, s13742-015-0080–0087. *https://doi.org/10.1186/s13742-015-0080-7*

24. Sayers, E.W., Beck, J., Bolton, E.E., Brister, J.R., Chan, J., Connor, R., Feldgarden, M., Fine, A.M., Funk, K., Hoffman, J., *et al.* (2024) Database resources of the National Center for Biotechnology Information in 2025, *Nucleic Acids Res* 53, D20–D29. *https://doi.org/10.1093/nar/gkae979*

25. Brettin, T., Davis, J.J., Disz, T., Edwards, R.A., Gerdes, S., Olsen, G.J., Olson, R., Overbeek, R., Parrello, B., Pusch, G.D., *et al.* (2015) RASTtk: A modular and extensible implementation of the RAST algorithm for building custom annotation pipelines and annotating batches of genomes, *Sci Rep* 5, 8365. *https://doi.org/10.1038/srep08365*

26. Cuccuru, G., Orsini, M., Pinna, A., Sbardellati, A., Soranzo, N., Travaglione, A., Uva, P., Zanetti, G., and Fotia, G. (2014) Orione, a web-based framework for NGS analysis in microbiology, *Bioinformatics* 30, 1928–1929. *https://doi.org/10.1093/bioinformatics/btu135*

27. Seemann, T. (2014) Prokka: rapid prokaryotic genome annotation, *Bioinformatics* 30, 2068–2069. *https://doi.org/10.1093/bioinformatics/btu153*

28. Blin, K., Shaw, S., Augustijn, H.E., Reitz, Z.L., Biermann, F., Alanjary, M., Fetter, A., Terlouw, B.R., Metcalf, W.W., Helfrich, E.J.N., *et al.* (2023) antiSMASH 7.0: new and improved predictions for detection, regulation, chemical structures and visualisation, *Nucleic Acids Research* 51, W46–W50. *https://doi.org/10.1093/nar/gkad344*

29. Tsugawa, H., Cajka, T., Kind, T., Ma, Y., Higgins, B., Ikeda, K., Kanazawa, M., VanderGheynst, J., Fiehn, O., and Arita, M. (2015) MS-DIAL: data-independent MS/MS deconvolution for comprehensive metabolome analysis, *Nat Methods* 12, 523–526. *https://doi.org/10.1038/nmeth.3393*

30. Samples, R.M., Puckett, S.P., and Balunas, M.J. (2023) Metabolomics Peak Analysis Computational Tool (MPACT): An Advanced Informatics Tool for Metabolomics and Data Visualization of Molecules from Complex Biological Samples, *Anal Chem* 95, 8770–8779. *https://doi.org/10.1021/acs.analchem.2c04632*

31. Wang, M., Carver, J.J., Phelan, V.V., Sanchez, L.M., Garg, N., Peng, Y., Nguyen, D.D., Watrous, J., Kapono, C.A., Luzzatto-Knaan, T., *et al.* (2016) Sharing and community curation of mass spectrometry data with GNPS, *Nat Biotechnol* 34, 828–837. *https://doi.org/10.1038/nbt.3597*

32. Pu, H., Jiang, T., Peng, D., Xia, J., Gao, J., Wang, Y., Yan, X., Huang, X., Duan, Y., and Huang, Y. (2022) Degradation of mirubactin to multiple siderophores with varying Fe(III) chelation properties, *Org Biomol Chem* 20, 5066–5070. *https://doi.org/10.1039/D2OB00942K*

33. Montreemuk, J., Stewart, T.N., and Prapagdee, B. (2024) Bacterial-assisted phytoremediation of heavy metals: Concepts, current knowledge, and future directions, *Environmental Technology & Innovation* 33, 103488. *https://doi.org/10.1016/j.eti.2023.103488*

34. Wang, S., Wang, J., Zhou, Y., Huang, Y., and Tang, X. (2022) Prospecting the plant growth–promoting activities of endophytic bacteria Franconibacter sp. YSD YN2 isolated from *Cyperus esculentus* L. var. sativus leaves, *Annals of Microbiology* 72, 1. *https://doi.org/10.1186/s13213-021-01656-2*

35. PanReac AppliChem Marine Agar (Dehydrated Culture Media) for microbiology,

36. Heffernan, J.R., Wildenthal, J.A., Tran, H., Katumba, G.L., McCoy, W.H., and Henderson, J.P. (2024) Yersiniabactin is a quorum-sensing autoinducer and siderophore in uropathogenic *Escherichia coli*, *mBio* 15, e0027723. *https://doi.org/10.1128/mbio.00277-23*

37. Khan, M., Bhargava, P., and Goel, R. (2019) Quorum Sensing Molecules of Rhizobacteria: A Trigger for Developing Systemic Resistance in Plants. In Plant Growth Promoting Rhizobacteria for Sustainable Stress Management : Volume 1: Rhizobacteria in Abiotic Stress Management, R. Z. Sayyed, N. K. Arora, and M. S. Reddy, eds. (Springer), pp. 117–138. *https://doi.org/10.1007/978-981-13-6536-2_7*

38. Sultana, S., Alam, S., and Karim, M.M. (2021) Screening of siderophore-producing salt-tolerant rhizobacteria suitable for supporting plant growth in saline soils with iron limitation, *Journal of Agriculture and Food Research* 4, 100150. *https://doi.org/10.1016/j.jafr.2021.100150*

39. C. Sarathambal, P.J. Khankhane, and D.K. Singh (2015) Characterization of metal tolerant and plant growth promoting rhizobacteria colonizing in weed rhizosphere, *Weed Science for Sustainable Agriculture, Environment and Biodiversity* 1, 4.

40. Taheri, Y., Herrera-Bravo, J., Huala, L., Salazar, L.A., Sharifi-Rad, J., Akram, M., Shahzad, K., Melgar-Lalanne, G., Baghalpour, N., Tamimi, K., *et al.* (2021) *Cyperus spp.*: A Review on Phytochemical Composition, Biological Activity, and Health-Promoting Effects, *Oxidative Medicine and Cellular Longevity* 2021, 4014867. *https://doi.org/10.1155/2021/4014867*

41. Ventura, M., Canchaya, C., Tauch, A., Chandra, G., Fitzgerald, G.F., Chater, K.F., and Sinderen, D. van (2007) Genomics of Actinobacteria: Tracing the Evolutionary History of an Ancient Phylum, *Microbiology and Molecular Biology Reviews : MMBR* 71, 495. *https://doi.org/10.1128/MMBR.00005-07*

42. Giessen, T.W., Franke, K.B., Knappe, T.A., Kraas, F.I., Bosello, M., Xie, X., Linne, U., and Marahiel, M.A. (2012) Isolation, Structure Elucidation, and Biosynthesis of an Unusual Hydroxamic Acid Ester-Containing Siderophore from *Actinosynnema mirum, J Nat Prod* 75, 905–914. *https://doi.org/10.1021/np300046k*

43. Chakraborty, K., Kizhakkekalam, V.K., Joy, M., and Chakraborty, R.D. (2022) Bacillibactin class of siderophore antibiotics from a marine symbiotic *Bacillus* as promising antibacterial agents, *Appl Microbiol Biotechnol* 106, 329–340. *https://doi.org/10.1007/s00253-021-11632-0*

44. Timofeeva, A.M., Galyamova, M.R., and Sedykh, S.E. (2022) Bacterial Siderophores: Classification, Biosynthesis, Perspectives of Use in Agriculture, *Plants* 11, 3065. *https://doi.org/10.3390/plants11223065*

45. Kepplinger, B., Wen, X., Tyler, A.R., Kim, B.-Y., Brown, J., Banks, P., Dashti, Y., Mackenzie, E.S., Wills, C., Kawai, Y., *et al.* (2022) Mirubactin C rescues the lethal effect of cell wall biosynthesis mutations in *Bacillus subtilis*, *Front Microbiol* 13. *https://doi.org/10.3389/fmicb.2022.1004737*

46. Dimopoulou, A., Theologidis, I., Benaki, D., Koukounia, M., Zervakou, A., Tzima, A., Diallinas, G., Hatzinikolaou, D.G., and Skandalis, N. (2021) Direct Antibiotic Activity of Bacillibactin Broadens the Biocontrol Range of *Bacillus amyloliquefaciens* MBI600, *mSphere* 6, e0037621. *https://doi.org/10.1128/mSphere.00376-21*

47. Agathokleous, E., Zhou, B., Geng, C., Xu, J., Saitanis, C.J., Feng, Z., Tack, F.M.G., and Rinklebe, J. (2022) Mechanisms of cerium-induced stress in plants: A meta-analysis, *Science of The Total Environment* 852, 158352. *https://doi.org/10.1016/j.scitotenv.2022.158352*

48. Khan, A.M. (2017) Accumulation, uptake and bioavailablility of rare earth elements (REES) in soil grown plants from ex-mining area in Perak, Malaysia, *Appl Ecol Env Res* 15, 117–133. *https://doi.org/10.15666/aeer/1503_117133*

49. Fiedler, H.-P., Krastel, P., Müller, J., Gebhardt, K., and Zeeck, A. (2001) Enterobactin: the characteristic catecholate siderophore of Enterobacteriaceae is produced by *Streptomyces* species, *FEMS Microbiology Letters* 196, 147–151. *https://doi.org/10.1111/j.1574-6968.2001.tb10556.x*

50. Reshetnikov, A.S., Khmelenina, V.N., Mustakhimov, I.I., and Trotsenko, Y.A. (2011) Genes and Enzymes of Ectoine Biosynthesis in Halotolerant Methanotrophs. In Methods in Enzymology (Elsevier), pp. 15–30. *https://doi.org/10.1016/B978-0-12-386905-0.00002-4*

51. Zhao, B., Lin, X., Lei, L., Lamb, D.C., Kelly, S.L., Waterman, M.R., and Cane, D.E. (2008) Biosynthesis of the Sesquiterpene Antibiotic Albaflavenone in *Streptomyces coelicolor* A3(2) *, *Journal of Biological Chemistry* 283, 8183–8189. *https://doi.org/10.1074/jbc.M710421200*

52. Deflandre, B., Stulanovic, N., Planckaert, S., Anderssen, S., Bonometti, B., Karim, L., Coppieters, W., Devreese, B., and Rigali, S. (2022) The virulome of *Streptomyces scabiei* in response to cello-oligosaccharide elicitors, *Microbial Genomics* 8, 000760. *https://doi.org/10.1099/mgen.0.000760*

ABOUT STUDENT AUTHOR

Phoebe Dennison is currently a chemistry and Spanish double major at Smith College. She completed this research for a chemical ecology course (CHM 350; Chemical Ecology: Catch Fe If You Can) but continues to conduct research in other areas of chemistry. She currently does surface chemistry research with Professor Kate Queeney in the Department of Chemistry. Phoebe will graduate in the spring of 2026 and plans to pursue a career in human health.

PRESS SUMMARY

Plants and root-associated microbes can be used to clean up heavy metal-contaminated environments using natural metal-binding molecules or siderophores. Some *Cyperus* plants have been reported to bind iron in wastewater, making them useful for cleaning up metal pollution. Herein, we examined whether siderophore-producing bacteria in the rhizosphere of *Cyperus virens*, an understudied member of this genus, could be used to treat metal pollution. Using an assay that changes color in the presence of siderophores, we isolated siderophore-producing bacteria. By analyzing their DNA, we discovered one of the bacteria was *Streptomyces* sp. PD-100-01 and contained genes that could make bioactive compounds, including siderophores. Furthermore, chemical analyses of *Streptomyces* sp. PD-100-01 cultures detected several catecholate siderophores, including mirubactin A and enterobactin. Together, these data suggest *C. virens* and its root-associated bacteria may be valuable tools for cleaning up metal pollution.